

A design project by students in the Department of Aerospace Engineering at Auburn University under the sponsorship of the NASA/USRA University Advanced Design Program.

Auburn University
Auburn University, Alabama
June 1990

(NASA-CR-186661) HIGH SPEED CIVIL TRANSPORT
(Auburn Univ.) 94 p CSCL OIC

N90-23396

Unclass
H2/05 0289196

HIGH SPEED CIVIL TRANSPORT

HIGH SPEED CIVIL TRANSPORT

SCOTT BOGARDUS
BRENT LOPER
CHRIS NAUMAN
JEFF PAGE
RUSTY PARRIS
GREG STEINBACH

ABSTRACT

The design process of the High Speed Civil Transport (HSCT) combines existing technology with the expectation of future technology to create a Mach 3.0 transport. The HSCT has been designed to have a range in excess of 6000 nautical miles and carries up to 300 passengers. This range will allow the HSCT to service the economically expanding Pacific Basin region. Effort has been made in the design to enable the aircraft to use conventional airports with standard 12,000 foot runways. With a takeoff thrust of 250,000 pounds, the four supersonic through-flow engines will accelerate the HSCT to a cruise speed of Mach 3.0. The 679,000 pound (at takeoff) HSCT is designed to cruise at an altitude of 70,000 feet, flying above most atmospheric disturbances.

Table of Contents

<u>Title</u>	<u>Page</u>
I. Abstract	iii
II. List of Symbols	vi
III. List of Figures	x
IV. List of Tables	xii
V. Introduction	1
VI. Configuration	6
VII. Materials	22
A. Performance	23
B. Costs	25
C. Disadvantages of composites	25
D. Material erosion	26
E. Specific material	27
F. Manufacturing methods	27
VIII. Structures	34
A. Heat critical regions	35
1. Nose cone	35
2. Wing and vertical tail leading edges	36

3. Engine cowl	36
4. Wing upper and lower panels	36
B. Heat noncritical regions	38
1. Wing internal structure	38
2. Fuselage	39
IX. Propulsion	40
A. Supersonic Through-flow Fan Engine Inlet Design	41
B. Supersonic Flow Fan	46
C. Core Inlet and Bypass Duct	49
D. Engine Core	49
E. Nozzle	50
F. Performance	51
G. Conclusion	52
X. Stability Analysis	61
XI. Flight Profile	67
XII. Summary and Conclusions	76
XIII. Bibliography	79

List of Symbols

<u>Symbol</u>	<u>Description</u>	<u>Units</u>
a	Acceleration	ft/sec ²
C_D	Drag Coefficient	-
C_{D0}	Parasite Drag Coefficient	-
C_L	Lift Coefficient	-
C_{Lmax}	Maximum Lift Coefficient	-
C_M	Moment Coefficient	-
c	Chord Length	ft
\bar{c}	Mean Aerodynamic Chord	ft
c_p	Specific Heat	BTU/lbm°F
D	Drag	lb
D_{TO}	Drag at Takeoff	lb
E	Span Efficiency Factor	-
F	Force Applied	lb
F_b	Force due to Braking	lb
F_c	Drag Force at Contact	lb
F_s	Static Force	lb

F_{TO}	Force at Takeoff	lb
g	Gravity	ft/sec ²
h	Height	ft
L	Lift	lb
L/D	Lift-Drag Ratio	-
M	Mach Number	-
m	Mass	lbm
\dot{m}	Mass Flow Rate	lbm/sec
n	Load Factor	-
R	Gas Constant	ftlb/lbmR
Re	Reynold's Number	ft ²
S_{WET}	Wetted Area	ft ²
S_{TOTAL}	Roll Distances	ft
T	Thrust	lb
T_{AV}	Thrust Available	lb
T_{REQ}	Thrust Required	lb
T_{REV}	Reverse Thrust	lb
T_{TO}	Thrust at Takeoff	lb

TSFC	Thrust Specific Fuel Consumption	lbm/hr-lb
t	Time	sec
t / c	Thickness to Chord Ratio	-
V	Velocity	ft/sec
V _{avg}	Average Velocity	ft/sec
V _{CL}	Climb Velocity	ft/sec
V _{LO}	Velocity at Lift-off	ft/sec
V _b	Velocity at Braking	ft/sec
V _c	Velocity at Touchdown	ft/sec
V ₅₀	Velocity to Clear 50' Obstacle	ft/sec
W	Weight	lb
W _e	Empty Weight	lb
W _o	Takeoff Weight	lb
W _f	Final Weight	lb
W/S	Wing Loading	lb/ft ²
X	Distance	ft
X _{cg}	Center of Gravity Location	ft
γ	Specific Heat Ratio	ftlb/lbmR

Δ	Change	-
α	Sweep Angle	degrees
λ	Taper Ratio	-
ρ	Density	slugs/ft ³

List of Figures

<u>Figure</u>	<u>Description</u>	<u>Page</u>
1	Basic Configuration of the HSCT	15
2	Vorticity Created by the Forward Delta	16
3	Schematic of the Double Wedge Airfoil	16
4	Schematic of the Engine Exhaust	17
5	Configuration of the Fuel System	18
6	Inboard Configuration	19
7	Comparison of Fatigue Characteristics	31
8	Comparison of Corrosion Characteristic	32
9	Vacuum Bagging Package	32
10	Schematic of the Supersonic Through-flow Fan Engine	54
11	Supersonic Through-flow Fan Inlet	55
12	Flow Velocity Relative to the Fan Blade	55
13	Thrust Specific Fuel Consumption Variation with Specific Thrust at Sea Level and Different Combuster Temperatures (Bypass Ratio = 1.5)	56

14	Thrust Specific Fuel Consumption Variation with Specific Thrust at Sea Level and Different Combuster Temperatures (Bypass Ratio = 2.0)	57
15	Thrust Specific Fuel Consumption Variation with Specific Thrust at Sea Level and Different Combuster Temperatures (Bypass Ratio = 2.5)	58
16	Thrust Specific Fuel Consumption at an Altitude of 45,000 feet and at Different Values of Bypass Ratios	59
17	Thrust Specific Fuel Consumption at an Altitude of 70,000 feet and at Different Values of Bypass Ratios	60
18	Flight Profile of the HSCT	75

List of Tables

<u>Table</u>	<u>Description</u>	<u>Page</u>
1	Dimension of the HSCT	20
2	Drag Polars at Various Flight Speeds and Altitudes	21
3	Comparison of Material Waste	33

INTRODUCTION

The current increase in worldwide passenger travel dictates that a more efficient means of air transportation be developed. During the past two decades , the countries of the Asian Pacific Rim, which include Japan, Hong Kong, Singapore, South Korea, Taiwan, Indonesia, Malaysia, the Philippines, Thailand and the People's Republic of China, have made considerable progress toward becoming major centers of world economic activity. Not only is Japan the second largest economic power in the world, but even the countries recording low economic growth within the Pacific Rim have far outpaced the economic growth of the United States and leading countries of Western Europe. If this growth continues over the next two decades, the Pacific Rim nations could become the economic power center of the world.

The tremendous economic growth of the Pacific Rim has resulted in an increase in air travel to and from the region. Based on historical trends in airline traffic, the region's premier economic growth and the emerging growth potential of the Chinese and Indian air transport markets, the Asia-Pacific region has often been characterized as the "future dynamo" of the international civil

aviation industry. Asian markets now account for 41 percent for worldwide air traffic on flights of over 5,000 miles. According to the Air Transport Association, America-Orient traffic should increase by 11 percent annually into the mid 1990's.

As travel and trade with the Pacific Rim nations increase more productive forms of air travel will be needed. Currently, the flight time between the United States and the Pacific Rim ranges from 10 to 16 hours. A flight of this length is a waste of valuable time, and results in severe jet lag; this is a considerable problem for business travellers who comprise a large portion of the U.S.-Pacific Rim travel. Reducing trans-Pacific flight times to a more reasonable four or five hours would be a major step in relieving the problem now associated with trans-Pacific travel. Considering the projected growth in the economies of the Pacific Rim, and the corresponding growth in air travel to the region, it is apparent that a quicker, more efficient means of travel will be needed to meet the demands of the increasing air travel market. The High Speed Civil Transport is a stepping stone for the United States to maintain a hold on the commercial aircraft industry.

There are several structural, propulsion, and material problems to designing the HSCT. The aircraft structure must be designed to be of minimal weight, and yet be able to support the engines and engine housing, the fuel load, and the payload. The advantages of weight, strength, heat resistance and durability of composites is evident over that of aluminum; thus composite material is chosen whenever practical. Using the lightweight material of composites reduces the total takeoff weight and will decrease the thrust required for takeoff.

A flight profile for the HSCT must be designed to attain cruise speeds as quickly as possible. The fuel and lift requirements are drastically reduced once the aircraft has attained cruise altitude and cruise speed. To obtain the flight plan for the HSCT, a flight profile must be established which will increase the range of flight and improve airplane efficiency.

Stability analysis of the HSCT will be difficult because of the wide range of speeds. The aircraft's aerodynamic center is affected by different flow regimes and the control characteristics will change through different mach regimes. Approximations of the

aerodynamic center and theoretical center of gravity locations must be fairly accurate to ensure stability and controllability throughout all flight regimes.

HIGH SPEED CIVIL TRANSPORT

CONFIGURATION

The development of today's HSCT must incorporate favorable flight characteristics in both the supersonic and subsonic regimes. The HSCT is designed to carry 300 passengers at high-altitude cruise speeds of Mach 3 over a range of approximately 6000 miles. Overall, the HSCT must incorporate its best characteristics in supersonic flight because it is in this regime the aircraft will spend most of its time. Some important subsonic properties desired are sufficient lift for takeoffs and landings at conventional airports and the ability to handle the various loads generated during flight. Most of all, in both the subsonic and supersonic flight regimes drag must be kept to a minimum. The proposed configuration is shown in Figure 1 and its dimensions are given in Table 1.

Wing Design

In the design of wing characteristics, one of the most important aspects is the determination of the shape of the airfoil. Due to the high speeds in which the HSCT will be flying, conventional airfoils cannot be used. The double wedge airfoil is most promising. The double wedge, due to its sharp leading edge, will cause the flow to

separate from the airfoil at low angles of attack in the subsonic flight regime. This separation causes a decrease in the lift coefficient obtainable in subsonic flight. But because of the large wing area the wing creates a large amount of lift. Therefore, the criteria governing the type of airfoil to use is the amount of drag created during the flight. This is the main reason for the selection of the double wedge airfoil.

For the design of the HSCT, two configuration types were considered, the variable-sweep wing and the double delta. When determining the configuration type it is important to keep in mind the lift-drag ratio, low speed handling, performance, stability, and control of the aerodynamic center. The control of the aerodynamic center is a primary concern because the center of lift moves a large distance aft between the subsonic and supersonic regimes. By using a variable-sweep wing, the shift of the aerodynamic center can be controlled rather easily because of the wing's ability to move in flight. Even though the variable-sweep wing gives good control of the aerodynamic center it yields several drawbacks in the areas of complexity, low speed handling, stability, control, weight, and cost. Due to the drawbacks of the variable-sweep wing another

configuration is desired.

The most promising configuration is the double-delta wing. The double-delta will meet the requirements for supersonic speeds and achieve excellent low speed characteristics, but does not give the control of the aerodynamic center needed. The control of the aerodynamic center will be achieved by shifting fuel aft to compensate for the move of the center of lift. The HSCT will use a double-delta wing configuration (Fig. 1) with the dimensions given in Table 1.

The double-delta's large size provides a high lift system with low wing loading making takeoff and landing speeds comparable to current subsonic jets. Also, the large sweep angles reduce the wing drag considerably and reduces the slope of the lift curve. The double-delta eliminates the need for slots, slats, trailing edge flaps and other artificial stability device. The simplicity of the double-delta wing reduces the weight, economic, and maintenance factors. A unique characteristic of the double-delta wing in subsonic flight is that vortices generated by the forward delta wing will sweep over the main delta removing the boundary layer from the wing (Fig. 2). Since the boundary layer is removed from a major portion of the

wing chances of stall are considerably reduced at high angles of attack.

Fuselage Design

The fuselage is a 300 foot long, cylindrical, slender body with a diameter of 15 feet. It is comprised of a passenger compartment and small fuel compartment. The passengers compartment is designed for 300 passengers. The compartment is 220 feet long and has an inside diameter of 11.5 feet. There are 61 rows of seats. For the most part the seating arrangement will be five abreast with an allotment of 34 inch seat spacing and 24 inch seat width. An 18 inch aisle will divide the five seats by having two on one side and three on the other. Windows will be aligned with the seats allowing the passengers a spectacular view during supersonic flight. Two entrances are provided, one in the front of the aircraft and one in the middle, each six feet in height. The floor for the passenger compartment will be three feet from the bottom of the fuselage. Some of the space created will be used for the passenger baggage and fuel storage.

The rear portion of the HSCT will have one vertical tail and no

horizontal tail. The reason for not having a horizontal tail is that having an all wing design will result in lower drag, higher lift to drag ratio, and lower structural weight. The vertical tail is 20.25 feet high and 52.6 feet long. Also, like the wings the vertical tail will be a double wedge airfoil with its maximum thickness of 3% of the chord and located at 50% of the chord. The leading edge has a sweep angle of 30.7 degrees and a trailing edge of 53.7 degrees.

At the front of the aircraft a tilt nose will be used. The tilt nose can be moved/tilted 14 degrees during flight depending on the flight regime. During takeoffs, landings, and subsonic flight the nose will be tilted downward to give the pilot superior visibility. As the aircraft approaches cruise speed, the nose will be moved to a more streamline position to minimize drag and decrease the flight station noise.

A special landing gear configuration will be needed to ensure that existing runways can support the weight of the HSCT. The proposed configuration will consist of the main landing gear which is a three strut arrangement with six wheels per strut. Two of these struts are wing mounted and the third is mounted down the centerline of the fuselage. The nose gear has two wheels and is mounted down the

centerline of the fuselage directly behind the tilt nose. The landing gear is designed to be completely retracted into the fuselage during flight.

The powerplant of the HSCT will consist of four through-flow fan engines. These engines are isolated from each other and from the passenger cabin (Fig. 4). The inner most engine on either side will be ten feet from the fuselage and its inlet is 67 feet from the leading edge of the wing. The outer engines are 25 feet from the fuselage and 35 from the leading edge. Due to this isolation, at supersonic speeds the shock waves generated at the engine inlets will not enter adjacent inlets. The engine locations serve to minimize noise and structural damage from both the forward and reverse jet wakes. Also, the location with respect to the fuselage will lessen the noise level in the cabin and improve internal environment and sonic fatigue. Finally, the engine inlets are located well behind the leading edge of the wing so the wing can shield the inlet from changes in the angle of inflow during maneuvers.

Due to the range for a trans-pacific flight and the amount of thrust required from the engines to carry a large payload, a substantial amount of fuel will be needed. The location of this fuel

is very important in the stability of the HSCT. Since the wing is relatively short spanwise and long chordwise, the fuel must be stored longitudinally, not laterally like most conventional airliners. Therefore as fuel is burned, it will have to be strategically taken out of the system so it will minimize the affect on the location of the center of gravity. The proposed configuration of the fuel system is shown in Figures 5 and 6. The areas shaded are the locations for the fuel tanks. The other areas are for the baggage and landing gears.

The gross takeoff weight of the HSCT is 679,000 pounds. As stated earlier, a primary concern in the design of a supersonic transport, such as the HSCT, is keeping the drag minimum. Drag polars were developed for the HSCT at various Mach numbers and various altitudes. The development of the drag polars up to Mach 2.0 were developed through the use of a Kern International BASIC aircraft performance program by Sidney A. Powers. The program was used for subsonic and low supersonic speeds. To obtain the drag polars for higher supersonic speeds, a method in Supersonic Airplanes and Winged Missles was used. It is noted that the drag at the higher supersonic Mach numbers is a function of the speed at

which the HSCT is traveling at the time. Table 2 shows the drag polars derived for the HSCT. Through the use of these drag polars the drag at any time during flight can be determined. Also, by using these drag polars and an ACSL performance program the amount of thrust, weight, range, and time is determined.

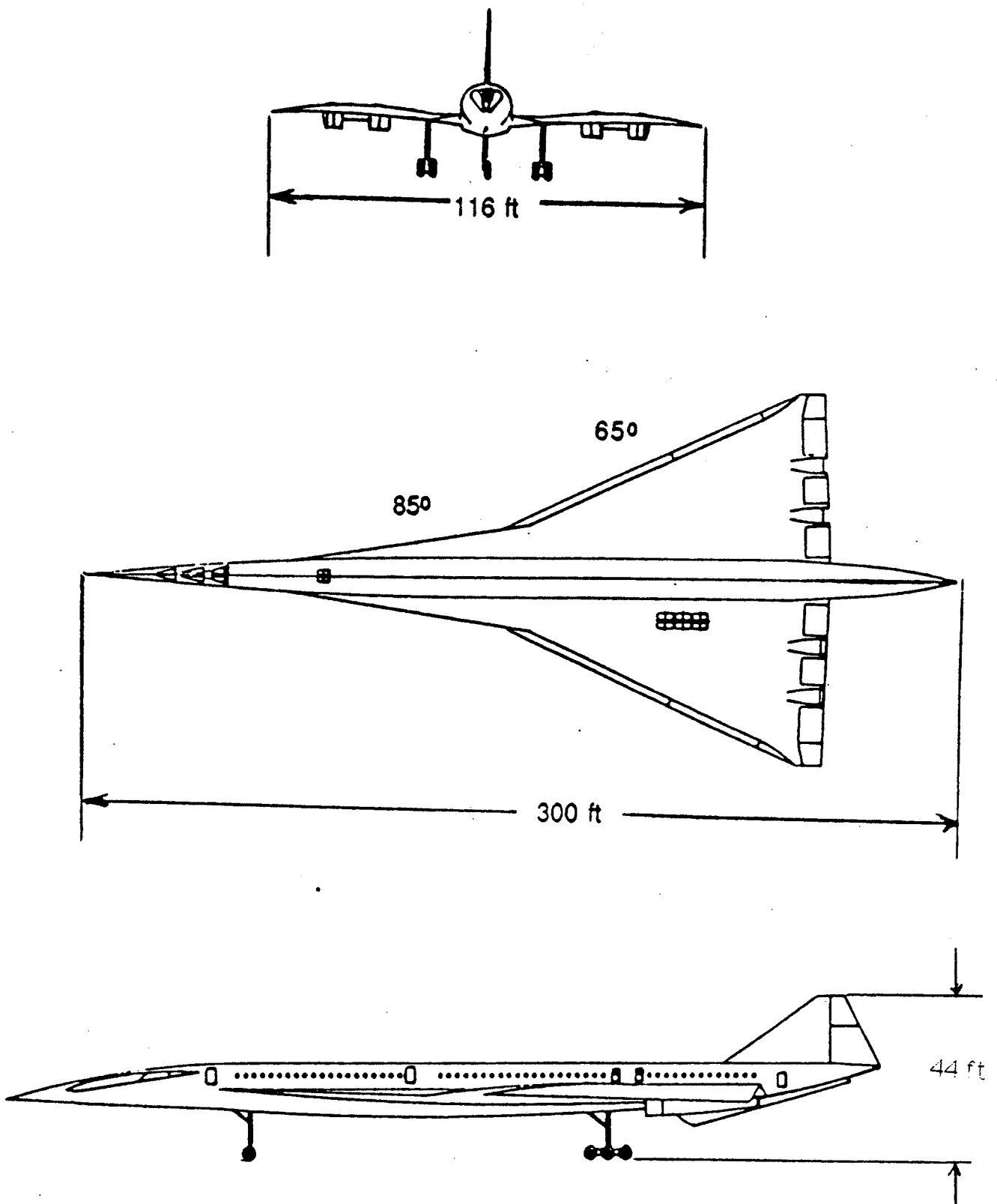


Figure 1. Basic Configuration of the HSCT

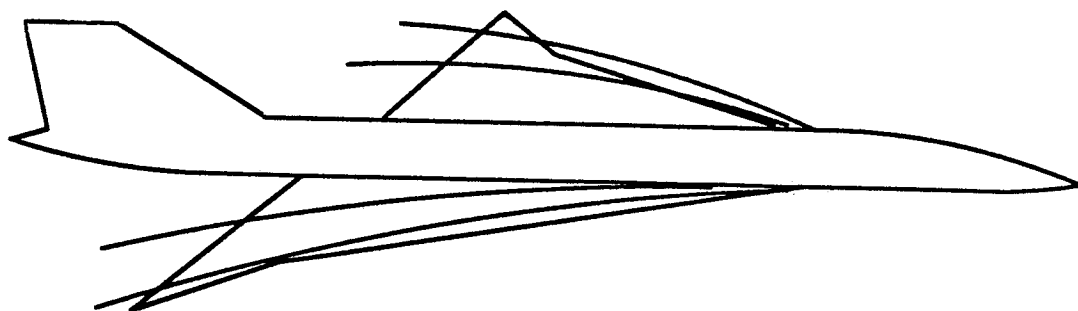


Figure 2. Vorticity Created by the Forward Delta

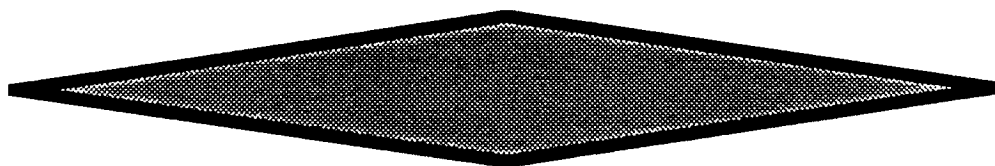


Figure 3. Schematic fo the Double Wedge Airfoil

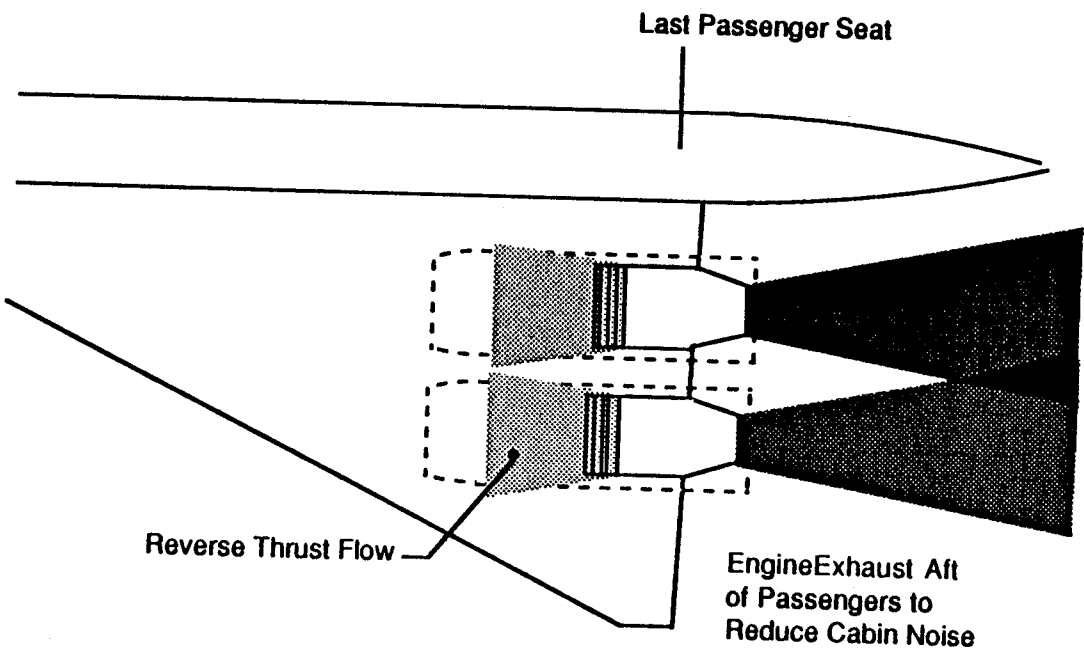


Figure 4. Schematic of the Engine Exhaust

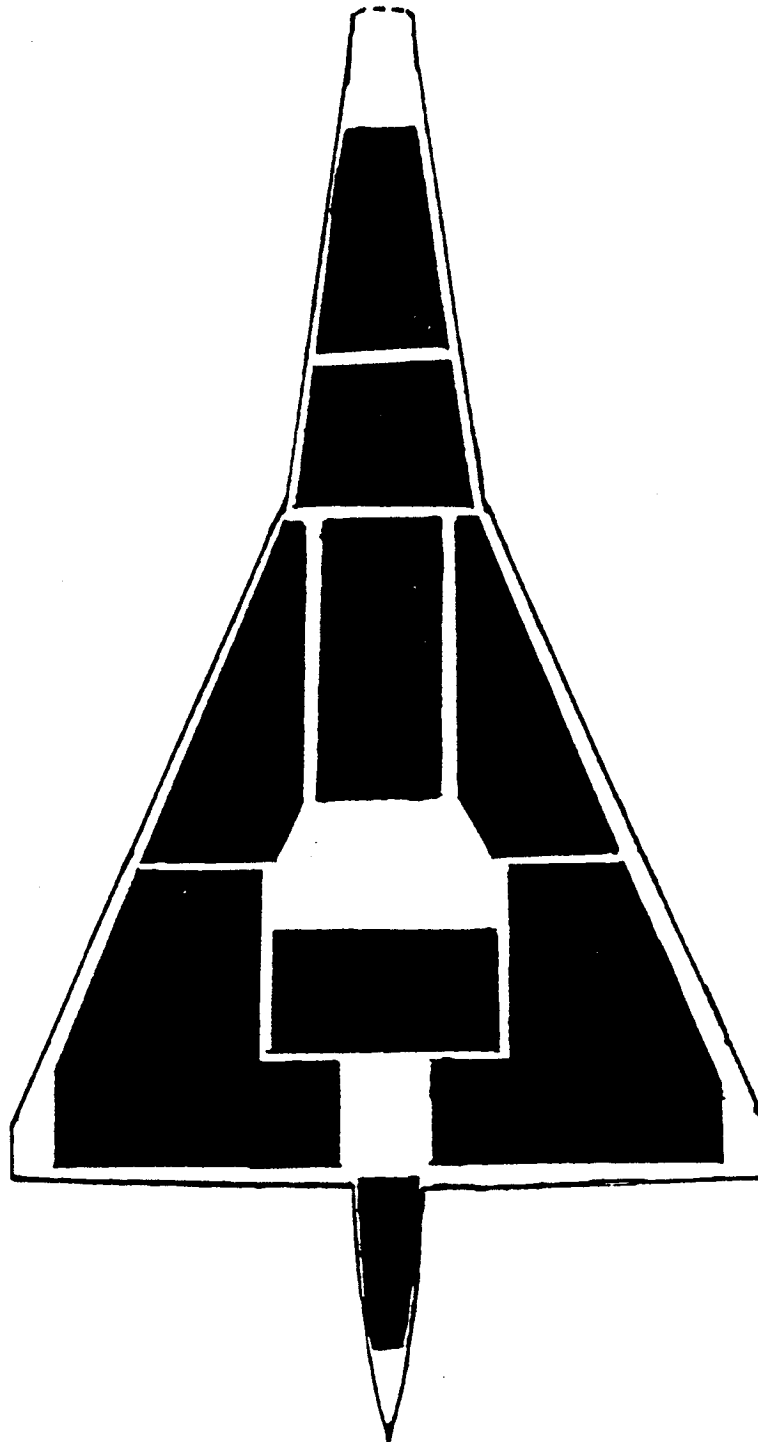


Figure 5. Configuration of the Fuel System

Figure 6. Inboard Configuration

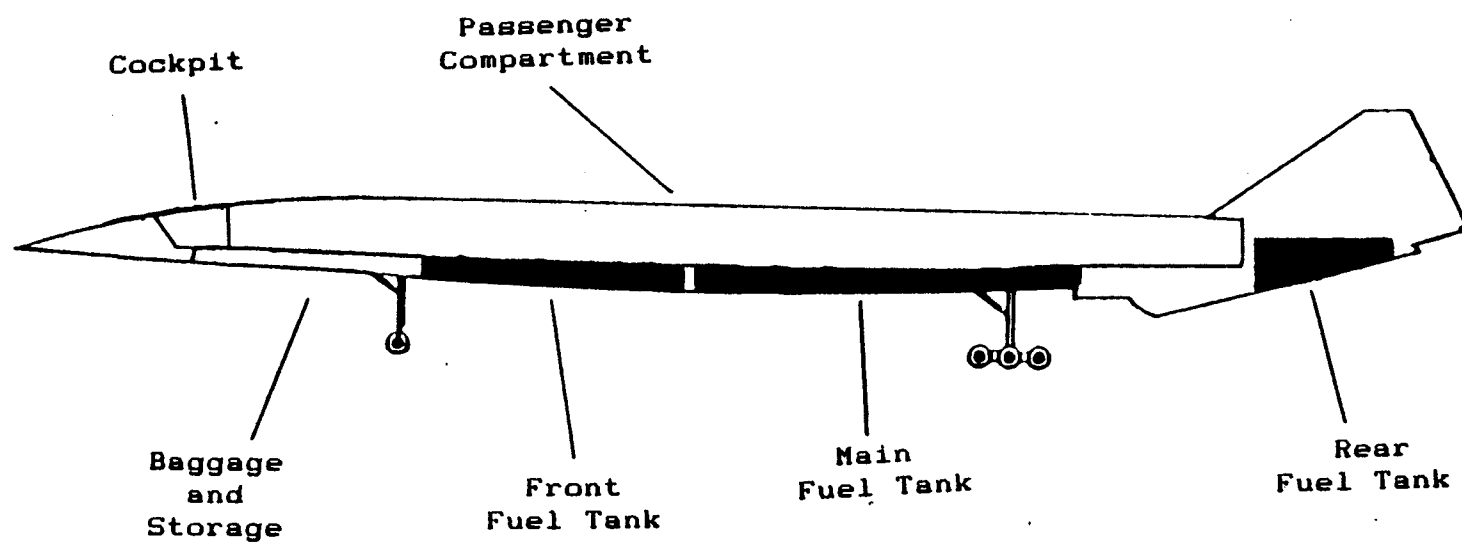


Table 1. Dimension of the HSCT

	<u>WING</u>	<u>TAIL</u>
Reference Wing Area	9556 ft ²	570.8 ft ²
Reference MAC	97 ft	35.2 ft
Span	116 ft	--
Aspect Ratio	1.41	--
Sweep Angles	Forward: 85° Main: 65°	Front: 30.7° Back: 53.7°
Root Chord	176 ft	52.6 ft
Tip Chord	0.0 ft	3.8 ft
Taper Ratio	0.00	0.07

Table 2. Drag Polars at Various Flight Speeds
and Altitudes

<u>Mach #</u>	<u>Altitude (ft.)</u>	<u>Drag Polar</u>	<u>(L/D)_{MAX}</u>
0.20	0.0	$C_D=0.00634+0.2423 C_L^2$	12.73
0.39	10,000	$C_D=0.00643+0.2402 C_L^2$	12.72
0.50	16,000	$C_D=0.0066+0.23970 C_L^2$	12.57
0.75	25,000	$C_D=0.00691+0.2379 C_L^2$	12.33
0.75	36,000	$C_D=0.0074+0.24250 C_L^2$	11.80
0.75	40,000	$C_D=0.0076+0.24510 C_L^2$	11.58
0.83	45,000	$C_D=0.00788+0.2465 C_L^2$	11.34
1.00	50,000	$C_D=0.00829+0.2456 C_L^2$	11.08
1.50	54,000	$C_D=0.01008+0.2335 C_L^2$	10.31
1.80	57,000	$C_D=0.01322+0.2196 C_L^2$	9.28
2-3	70,000	$C_D=0.01065/M+0.2941 C_L^2/M$	8.94

HIGH SPEED CIVIL TRANSPORT

MATERIALS

Material selection for the HSCT is a difficult task with the many new products on the market. The designer can choose from conventional aluminum and steel alloys, superalloys, and composites. Two key factors must be considered when deciding on a specific material. Generally, the most important is performance: strength, weight, thermal limits, electrical capabilities, etc. The second factor is cost. Cost is often a deciding factor between materials, particularly in the commercial aerospace industry where profit is the main motive.

With these points in mind, it has been decided that the HSCT will utilize continuously reinforced fiber composites as the main structural material. Reasons for this selection are categorized into the two interrelated groups mentioned, performance and cost.

PERFORMANCE

Continuously reinforced composites, as a whole, have superior strength and stiffness to weight ratios over most competitive metals. This translates directly into reduced operational costs as engine size and fuel requirements decrease with decreased aircraft

weight. Composites are thermally superior as well. High temperature composites such as carbon/carbon perform well up to 3000°F. Further, the continuous reinforcement can be tailored to pass a majority of the heat in almost any direction desired. The composite fibers, generally graphite, consist of tight covalent bonds which are excellent heat conductors. The matrix material is a poor heat conductor similar to the weak Van der Waals bonds between adjacent fibers. Thus, the fibers are aligned in the direction of heat flow desired, i.e. along the air flow. This alignment allows large quantities of heat to be transmitted back into the flow but not through the composite to the internal structure.

The ability to select fiber direction also carries significant structural benefits. The fiber is the load carrying element of the composite, while the matrix serves to evenly distribute loads between fibers and hold the fibers intact. Thus, by designing a part so that fibers are placed along specific known load paths, the overall amount of material is reduced, saving weight and raw material costs.

Two other performance characteristics should be mentioned. First, composites are more resistant to fatigue than metals, both

loading (Fig. 7) and sonic fatigue. Second, composites have improved corrosion resistance over metals which is especially important, given that the HSCT will be operating in a highly corrosive sea air environment (Fig. 8).

COSTS

Composites offer reduced costs over metals in several ways. Though more expensive per pound than metals, there is not nearly as much waste involved in part fabrication (Table 4). Overall manufacturing costs are lower for composites as well, because detailed parts can be made from simple tools in less time. No heavy machining or welding is needed, either.

DISADVANTAGES OF COMPOSITES

Some of the disadvantages of composites should also be pointed out:

1. Poor impact strength
2. Expensive facilities required (clean room, freezers, autoclaves, trained personnel, destructive and nondestructive testing equipment)

3. Difficult to interpret and sometimes repair defects

4. Stringent shelf life requirements

It is important to point out that by choosing an experienced composite manufacturer, a good deal of the costs incurred in (2),(3), and (4) can be avoided. Low impact strength is not a critical problem with civil aviation aircraft. In addition, unlike metals, overall cost of composite manufacturing continues to drop as technology advances and more is learned about composites.

MATERIAL EROSION

Material erosion due to collision with microscopic materials is another problem to be considered. Regions susceptible to this damage are the nose cone, all leading edges, and the cowl inlet. In these areas, an outer coating of silicon carbide will be applied to the composite. Silicon carbide is a high hardness, ablative ceramic, which, in impacts, will reflect heat and provide further heat protection.

SPECIFIC MATERIAL

Two particular types of composites have been chosen for

implementation on the HSCT, graphite/epoxy and carbon/carbon composites. Carbon/carbon composites are ultra high temperature and strength materials which will be used in heat sensitive areas. Graphite/epoxy composites, using a thermosetting plastic matrix, are lower temperature composites (900°F maximum temperature) but are very strong and relatively cheap. Graphite/epoxies will be used in areas that are not heavily affected by heat. The high cost of carbon/carbon composites prohibits their usage over the entire aircraft.

MANUFACTURING METHODS

The most widely used manufacturing method of carbon/carbon composites is a three step procedure called Resin Injection Molding. First, the carbon fibers are woven either onto a mandrel or a loom into a near net shape mesh. Next, the mesh, or mandrel, is placed into a mold and injected with resin. Finally, high pressure and temperature are applied to compact and cure the part. The finished product is an extremely strong, high temperature part with close dimensional tolerances.

Several methods will be used for graphite/epoxy manufacturing,

but by far the most useful is vacuum molding. The most effective method is an automated procedure which involves the use of preprogrammed machines to automatically lay preimpregnated, unidirectional sheets, commonly called tape, onto either a male or female tool. The stacks of tape, or laminate, are then cut at the edges automatically by a preprogrammed reciprocating saw with a diamond tipped blade (a.k.a. Gerber Cutter). Once this step is complete, the vacuum bagging package and vacuum bag (Fig. 9) are manually applied. Proper application of the vacuum bag package is the most important step in graphite/epoxy composite fabrication. A detail list of the vacuum bagging package is shown below and can be seen in reference to Figure 9.

1. Laminate, formed by automation
2. Porous material which will not adhere to the laminate during cure but will allow passage of excess resin as it is "squeezed" from the laminate during cure.
Usually a teflon coated fabric.
3. Bleeder, a porous material which soaks up excess resin from the laminate during cure.
4. Blocker, a nonporous thin film which does not all

resin passage and will not adhere to resin in the bleeder.

5. Breather, a .25-.50 inch thick loose random weave material which allows even distribution of the vacuum applied during cure.
6. Vacuum bag, a sealed, nonporous material which will cover the entire tool surface and internal vacuum bag package components. The vacuum bag will evenly distribute pressure to the laminate upon vacuum initiation.

Several important aspects of vacuum bagging must be noted here:

- No wrinkles or folds are allowed in the bleeder as this will produce small dents and ridges in the laminate surface. These defects can give rise to point stresses which may be high enough to cause failure.
- The entire part must be covered with the bagging package with as few overlaps or gaps as possible to ensure a quality part.

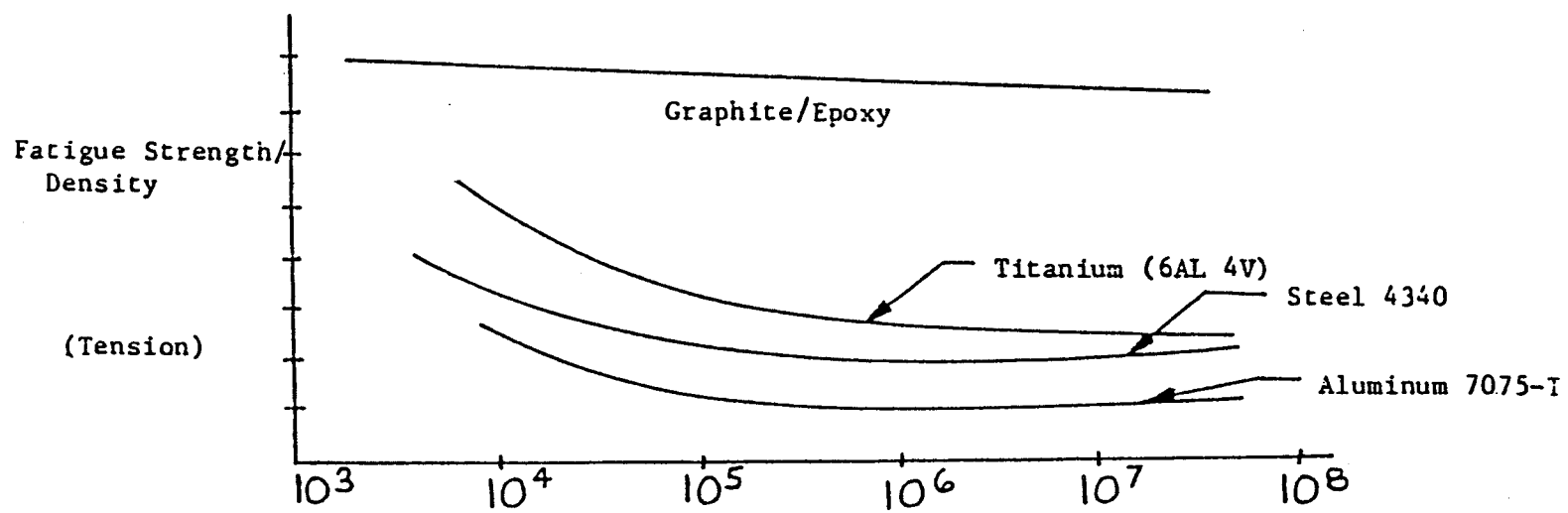
Once the vacuum bagging package has been applied vacuum ports

are inserted and the vacuum bag seal is tested for leaks ultrasonically. If sealed, the part is placed in an autoclave under increased temperature and pressure for cure.

The cure is essentially a three step process: liquification, compaction, and solidification. During liquification, the resin is heated until it becomes runny, like water. At this point, pressure is applied by the autoclave and through the vacuum ports squeezing excess resin from the laminate. Then it is soaked up by the bleeder. Careful control must be maintained during this stage of the cure as resin rich and resin starved composites must be trashed. Finally, during solidification, the temperature is increased to solidify the resin matrix. The part is then slowly cooled to avoid thermal shock and little additional machining is required.

Another popular graphite/epoxy forming technique is called pultrusion and is similar to both Resin Injection Molding and vacuum molding. First, fibers are pulled through a resin bath, or wetted, and then either wound onto a mandrel or pulled through a die in order to obtain the desired part. The part is then placed into a mold and cured in the same manner as above laminates.

Figure 7. Comparison of Fatigue Characteristics



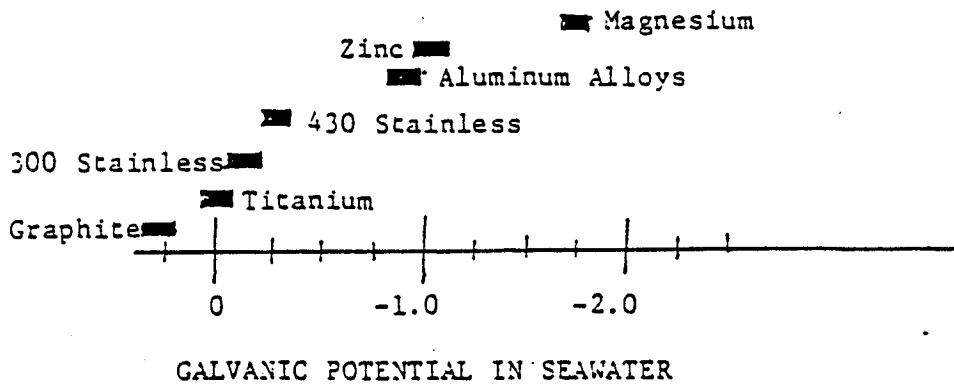


Figure 8. Comparison of Corrosion Characteristics

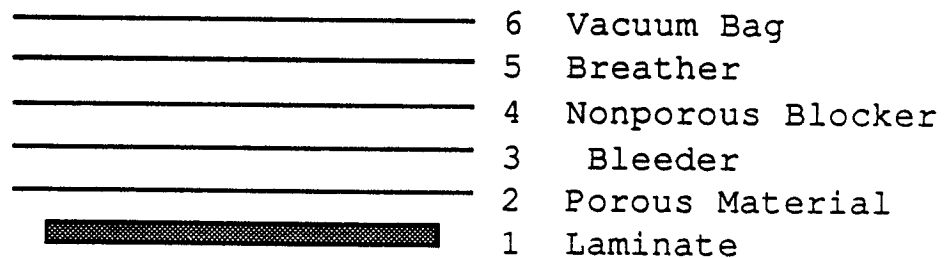


Figure 9. Vacuum Bagging Package

Table 3. Comparison of Material Waste

	<u>Finished Weight (lbs)</u> <u>of Components</u>	<u>Buy Weight (lbs)</u> <u>of Components</u>	<u>Percent of Raw</u> <u>Material Waste</u>
Aluminium	6,684	45,451	85
Steel	1,005	3,216	69
Titanium	4,567	50,885	91
Composites	182	237	23

HIGH SPEED CIVIL TRANSPORT

STRUCTURES

The discussion on structure is divided into two main parts, heat critical regions (carbon/carbon composites) and heat noncritical regions (graphite/epoxy composites).

HEAT CRITICAL REGIONS

Nose Cone

The HSCT nose cone is the most heat critical region on the aircraft. Ideally, the nose cone would come to a sharp point to minimize drag. However, a compromise must be made in rounding the nose cone tip to allow for material heat limitations. The sharpest nose cone radius allowable for the expected 850°F temperature is six inches. The material selection for the nose cone is a Resin Injection Method produced carbon/carbon composite with the majority of the fibers running along the nose cone's length. In addition, a heat blanket (backing insulation) will be used. The heat blanket will be a carbon whisker foam and is a bonded insert to the inside of the nose cone. The carbon whisker foam is effective because it consists of multidirectional Van der Waals bonds which

allow very little heat passage to the electronic equipment inside the cone.

Wing and Vertical Tail Leading Edges

The wing and vertical tail leading edges will also receive severe heating. Again, carbon/carbon composite will be used in conjunction with a thinner carbon whisker foam heat blanket to protect enclosed electrical, mechanical, and hydraulic equipment.

Engine Cowl

The engine cowl heat problem is the result of two forms of heating. The inlet is heated aerodynamically. Further aft, the cowl is heated by radiation from the engine combustion chamber and nozzle. Since it is not necessary to protect any kind of equipment, no heat blanket will be used. However carbon/carbon will again be utilized to withstand the high temperatures.

Wing Upper and Lower Panels

The increased velocity of air flowing past the wings causes substantial heating-up to 600°F due to skin friction. Thus,

carbon/carbon composites will be used for the wing panels with the upper fiber layers oriented in the flow direction to pass heat back into the stream. It should be noted that although some of the high temperature graphite/epoxy composites can withstand the expected temperatures, they would fail rather quickly. The reason behind this is that strength properties begin to degrade sufficiently for graphite/epoxy at such high temperatures. The effect is the lowering of safety factors and increasing susceptibility to massive fatigue failure. Carbon/carbon composite strength properties exhibit little change at this temperature and are thus better suited for the application.

There is a buildup that is a modification to the usual flat sheet/stringer arrangement employed in metal design. The buildup area in effect replaces the stringer and is a byproduct of effective composite design methods. This construction reduces structural complexity and assembly time by eliminating the number of parts required. Buildup sections run in the direction of the flow, fore to aft.

HEAT NONCRITICAL REGIONS

Wing Internal Structure

A conventional wing structure has been selected for the HSCT. This structure is commonly called the box structure and has proven quite effective at supporting heavy wing loading. The box structure consists of three main structural elements: spar, rib, and stiffened skin panel. Spars are an "I" cross section and run along the wing chords; they transmit wing loads to the fuselage and directly react the rearward pull of the wing due to drag. Composite spars are superior to metallic spars because they can be fabricated in one piece without material wastage using pultrusion. Length is limited only to autoclave size.

Ribs are basically stiffened flat panels with "T" flanges all around the edge. Cutouts in the flat panel are made where permissible to reduce weight. Ribs rest vertically in the structure and connect the wing upper and lower surfaces and spars. Again, composite construction eliminates the waste caused by matching metallic ribs. The stiffened skin Panel has already been discussed.

The box design has several important features. First, it is well suited for composites since the number of parts required and

easily analyzed compared to other competitive designs due to simple geometry. Third, the box design efficiently transmits shear and torque loads to the fuselage. Finally, the wing is almost entirely in tension, which is the strongest loading direction for composites. The vertical tail will also use the box design.

Fuselage

The fuselage skins will be slightly different from the wing skins in that they will be of sandwich construction. The circular "I" cross section can be easily made in two parts using pultrusion techniques. Certain sections of the aircraft cabin will permit the insertion of bulkheads. All bulkheads will be flat and of sandwich construction. New, large autoclaves will allow the bonding of skins to frames. The bonded sections will then be attached via a room temperature curing adhesive and mechanically fastened to each other. The floor support will be the standard box construction and warrants no elaboration. Floor boards will be of sandwich construction with a resin coated paper honeycomb.

HIGH SPEED CIVIL TRANSPORT

PROPULSION

The demands placed on the propulsion systems of future high speed civil transports must be met with new technology to increase efficiency and decrease weight. Designers have explored many new ideas for advanced engines with promising results. One of the most promising prospects is the supersonic through-flow fan engine (STFFE) (Fig. 10).

For this HSCT design, the STFF engine was chosen over other concepts because of its lighter weight, simpler fan, simpler turbomachinery, and the prospect of highly enhanced performance. The STFFE is a turbofan engine with a single stage fan without, in the case of this design, thrust augmentation. The STFFE is set apart from conventional turbofans because the fan-face Mach number is supersonic. Because the fan-face Mach number is supersonic, a long heavy inlet is not needed. This section will attempt to analyze the design and performance of the engine with a heavy reliance on technological advances in the fields of materials and aerodynamics.

STFFE INLET DESIGN

One of the major advantages of the STFFE is the much smaller,

thus lighter, inlet. Conventional turbofan engines must utilize long heavy inlets to slow the flow at the fan face. The flow energy in a conventional inlet is dissipated through a series of shocks. These shocks cause a decrease in pressure recovery which translates into a loss in overall engine efficiency. A high degree of boundary layer bleed in the inlet is also needed to prevent thermal choking due to viscous effects. In the conventional inlet, the flow must be slowed as efficiently as possible to a speed of Mach 1 at the throat of the inlet. The flow is then expanded to subsonic speeds before reaching the fan face. To accomplish subsonic expansion as efficiently as possible, the back pressure (static) at the fan face must be at or near some design point. This design point pressure is usually high while the dynamic pressure is reduced due to the reduced flow speed. The total pressure at the fan face is reduced from that at the mouth of the inlet by the extensive compression and expansion of the flow field. This pressure loss leads to decreased fan efficiency and a decrease in overall engine efficiency. The fan must also work harder to reach effective fan pressure ratios.

At off-design speeds, the conventional inlet experiences even further losses. Stronger shock waves are necessary to force the

flow to decelerate to Mach 1.0 at the inlet throat. The fan is forced to work at off-design pressures and rotational speeds. The results of off-design operation are further decreased pressure recovery due to stronger shocks, decreased fan pressure ratios, and overall engine efficiency losses. Programs directed at enhancing conventional turbofan operation have produced interesting ideas including variable geometry turbomachinery blades and variable geometry inlets, but the weight penalties are large. The STFFE inlet is much smaller than the conventional inlet. Since the flow is supersonic at the fan face, weaker shocks are needed to control and accelerate the flow. The inlet chosen for this design is variable geometry with variable capture area as well as variable throat area (Fig. 11). The variable geometry enables the engine to operate more efficiently at off-design speeds while the smaller size of the inlet keeps the weight penalties low.

At low, subsonic Mach numbers (0 to .5) the flow is accelerated to Mach 1.0 at the inlet throat and expanded to supersonic speeds at the fan face. At these speeds, the inlet cowling is extended forward to allow the flow to converge at the throat with a Mach number of one. The throat area is set relative to the inlet area to provide for

optimum supersonic flow conditions. At the throat, a weak normal shock occurs. This normal shock as well as viscous effects accounts for the total pressure loss over the entire length of the inlet. Since the flow travels a shorter distance in the STFFE inlet than in the conventional inlet, lower flow losses are realized and greater efficiency is achieved.

At a flight speed of Mach 1.0, the inlet cowling is retracted to provide for the minimum inlet area. Since the flow speed is already sonic, a minimum amount of compression is desired to reduce shock waves and pressure losses. The throat area is adjusted to provide for the most efficient supersonic expansion.

At higher Mach numbers, a bow shock forms at the point of the inlet core; a smaller shock forms on the lip of the inlet cowling. The inlet cowling is set to control the location of the wave and to prevent its movement into undesired locations (the throat area). The inlet area is adjusted to provide for optimum supersonic expansion.

At supersonic speeds, the flow field in the STFFE inlet does not have to be slowed to a Mach number of one at any point. Although the flow is slowed in the throat area, the pressure loss due to shocks is greatly reduced over conventional inlets. The higher flow speed does

induce more friction but the shorter inlet length reduces these effects. Boundary layer bleed can also be employed to reduce the frictional effects. The overall increase in pressure recovery translates into higher fan pressure ratios and higher compressor inlet pressures, both of which increase overall efficiency.

At the design point (Mach 3.0) the inlet cowl is positioned so the leading-edge bow wave of the inlet centerbody is attached to the cowl lip. This is to assure that the bow shock will not interfere with the airflow inside the inlet and to provide a more uniform flow deceleration. The throat area is opened to allow for the design fan-face Mach number.

The most notable advantage the STFFE inlet has over conventional inlets is the greatly reduced weight. With the aid of advanced materials, the STFFE inlet can be made lighter than with conventional materials. The STFFE inlet's smaller size also results in a substantial weight savings. The total estimated weight savings is 60% over conventional inlets. The estimated weight of the inlet and nacelle for this design is 2300 lb. This weight is an estimate due to the reliance on future developments in the materials field.

The inlet used in this design was developed by NASA Lewis

Research Center for a Mach 3.0 cruise engine. The centerbody is a simple conic section with a 13° half-angle. The inlet cowl translates forward or aft and the inlet throat area can constrict or expand. This area change is accomplished by moving the centerbody forward or aft.

SUPERSONIC FLOW FAN

The fan block of the STFFE consists of a single stage rotor and stator; the fan is made rugged to withstand the forces of supersonic flow. The fan is more the shape of a marine propeller than a conventional fan. There are many advantages and disadvantages predicted for this type fan. If the needed technology is developed, this radical new design will mean a significant increase in turbofan performance.

A major problem with the supersonic fan is the difficulty in determining the effects of the swirling, supersonic air on the efficiency of the compressor. The airflow at the compressor inlet is slowed to subsonic speeds with a diffuser. The complications come from analyzing the flow losses due to this diffusion and determining the optimum design for the diffuser. Another problem associated

with the unsteady, supersonic flow is the effect on the bypass stream. The bypass duct and core inlet are located aft of the fan. At this point, the flow is still supersonic. The formation of shock waves at this point is imminent, but the exact location and strength is difficult to determine. The problems listed above could have several adverse effects on engine performance; reduced efficiency and even compressor stall could result from a poorly designed diffuser, core inlet, or bypass duct. Advanced fan aerodynamic analysis must be developed to design the optimum system of fan, inlet and diffuser.

Another problem with the supersonic fan is not unique. The problem of fan blade flutter has been a major design challenge for all turbofan engineers. But the supersonic fan complicates the problem with supersonic axial flow. The vibration analysis for a long, slender (although highly rigid), rotating fan blade in supersonic flow is highly complicated, and is still further complicated by strong shock formations on the blades. Lighter, stronger, and more rigid material is needed to lessen the effects of the highly unsteady, swirling flow.

One advantage the supersonic fan has over the conventional fan is

a much more rugged construction. The STFFE fan is made to withstand the supersonic flow yet hold a weight advantage over conventional fan blocks. Many turbofan engines utilize multistage fan blocks to provide the necessary pressure ratio at supersonic speeds. These multistage fans are very heavy and complicated. The STFFE fan is simple in operation and relatively light. Again, lighter and stronger materials can improve this weight advantage and maybe simplify the analysis process.

Another advantage of the supersonic fan is the ease in controlling fan pressure ratio. In conventional turbofans, the angle of attack of the flow relative to the fan blades increases with increasing pressure ratio (Fig. 12). The back pressure aft of the fan increases the work needed to compress the flow. As a margin of safety against stalling the fan blades, the pressure ratio must be kept about 20% below maximum. Much higher axial speeds at the STFFE fan face decrease the possibility of stall.

The axial component of the velocity relative to the fan blade is large enough to maintain a margin of safety against stall for a wide range of pressure ratios. This performance characteristic enables

the engine designer to have greater freedom to optimize the engines efficiency and power.

CORE INLET AND BYPASS DUCT

As discussed above, the bypass duct and core inlet are subject to highly unsteady supersonic flow. To help control the flow in this region and to control bypass ratio, the core inlet is variable geometry. The core inlet has a sliding shroud that can translate fore and aft to vary the core inlet throat area to accommodate different incoming Mach numbers. By controlling the core airflow, the bypass flow can be controlled to some degree. This added control results in a decrease in spillage drag, more efficient bypass ratios for different flight speeds, and higher overall engine efficiency.

ENGINE CORE

The STFF engine core is basically the same as conventional turbofans. The incoming airflow is slowed to subsonic speeds before entering the compressor so the core remains primarily unaffected. The main difference between the STFFE and the conventional is advanced turbomachinery and lighter materials. For

more efficient operation and higher thrust, the combustor temperature is raised to very high values. New ceramics or other high temperature materials must be developed to allow these high operating values to be used. The turbine must be especially heat resistant in order to withstand the direct combustor exhaust in combination with high angular velocities.

More efficient core machinery and diffusers are also needed for an economically efficient design. The adiabatic efficiency factors, which are a measure of the loss in enthalpy with respect to the adiabatic case, approach a value of one with increasing efficiency. These values directly influence the thrust and thrust specific fuel consumption through the calculation of total temperature and total pressure difference across the different engine components. Better component design must be accomplished in order to increase these efficiencies to effective levels.

NOZZLE

The nozzle for this design was chosen to be fixed-geometry. The rear centerbody moves fore and aft in order to vary the nozzle throat

area. The translating centerbody is heavy but the simple and light nozzle compensates for the added weight.

PERFORMANCE

The performance of the STFFE is difficult to analyze due to the many unknowns in its operation (effects on the compressor, assumed efficiencies for the engine components, etc.). Most of the research directed at the STFFE has been done by NASA Lewis. The researchers at Lewis used the NNEP computer program to calculate the installed engine performance. For the analysis of this design, the thrust equation for conventional turbofans was used and the adiabatic efficiencies increased to reflect technological advances. The analysis was done using ACSL simulation language to model the HSCT over a 5600 nm. trip. The output consisted of thrust, thrust specific fuel consumption (TSFC), weight, air mass flow rate, thrust to weight ratio, combustor temperature and other aerodynamic or distance values. This simulation will be discussed later.

The program was modified to output specific thrust and thrust specific fuel consumption for plotting purposes. Figure 13 through Figure 15 are the plots made from this data. One observation that

specific thrust becomes independent of combustor temperature or bypass ratio as altitude increases. At 70000 ft. the values lie along the same line on the graph. At lower altitudes the variation is large with respect to both bypassed combustor temperature.

The range of the HSCT is affected by the lower weight and higher efficiency of the STFFE engines. Up to a 10% range increase could be realized by propulsion savings alone. This increase in range translates into longer and cheaper flights.

The speed and power requirements for the HSCT dictate that the fuel be able to withstand high temperatures for extended periods of time. A thermally stable jet fuel must then be used. The fuel JP-7 meets these requirements although it is expensive. Unless a lower priced, high temperature fuel is developed, JP-7 will be used. The cost and weight of actively cooling the fuel makes up for the extra cost of JP-7.

CONCLUSION

The future of the STFFE is very promising if further technological developments are made. The prospects for the use of the STFFE in

civil aviation are bright. Major engineering obstacles remain, but continuing research and development is making the concept a reality.

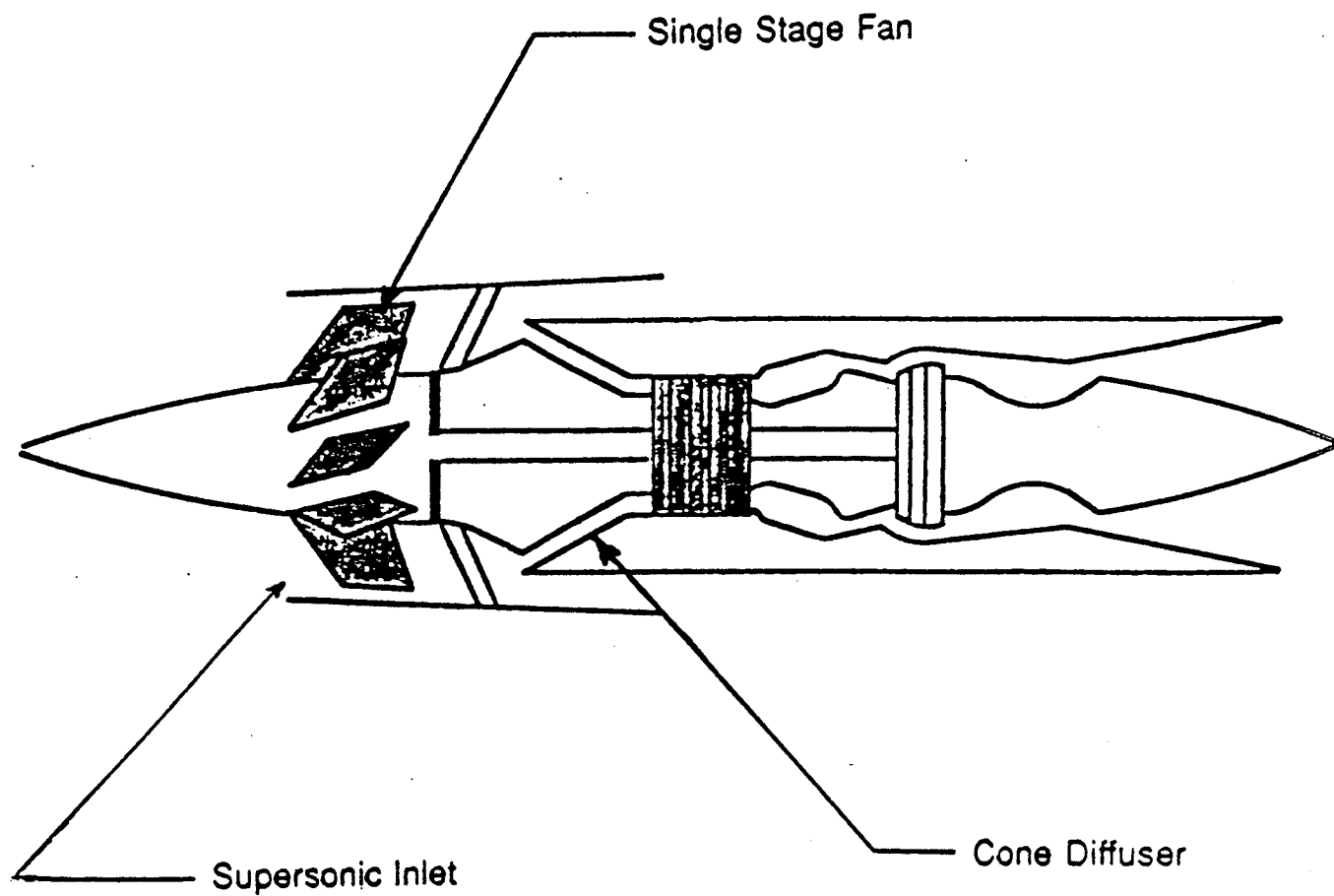


Figure 10. Schematic of the Supersonic Through-flow Fan

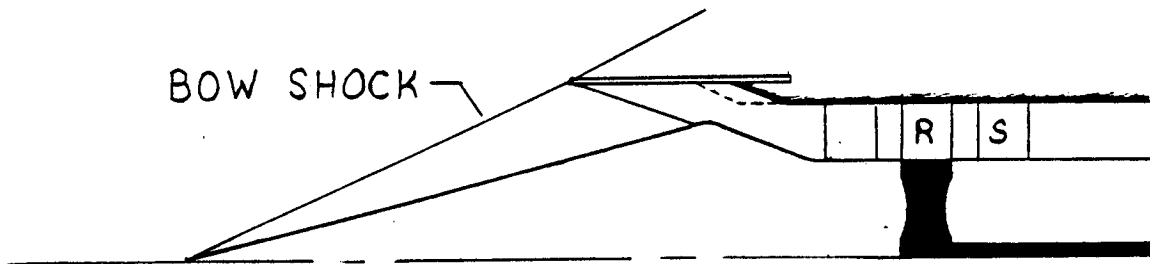
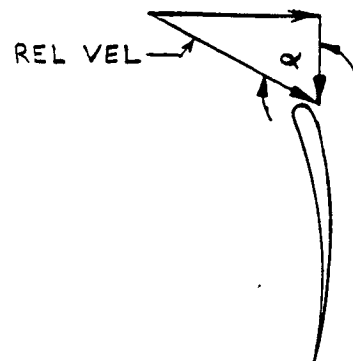
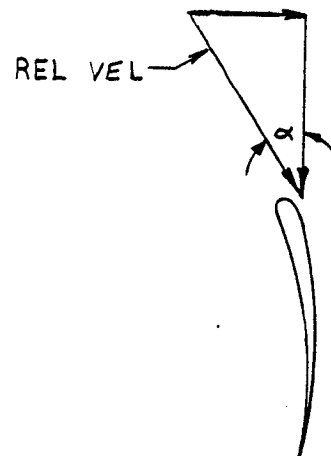


Figure 11. Supersonic Through-flow Fan Inlet



Conventional



STFFE

Figure 12. Flow Velocity Relative to the Fan Blade

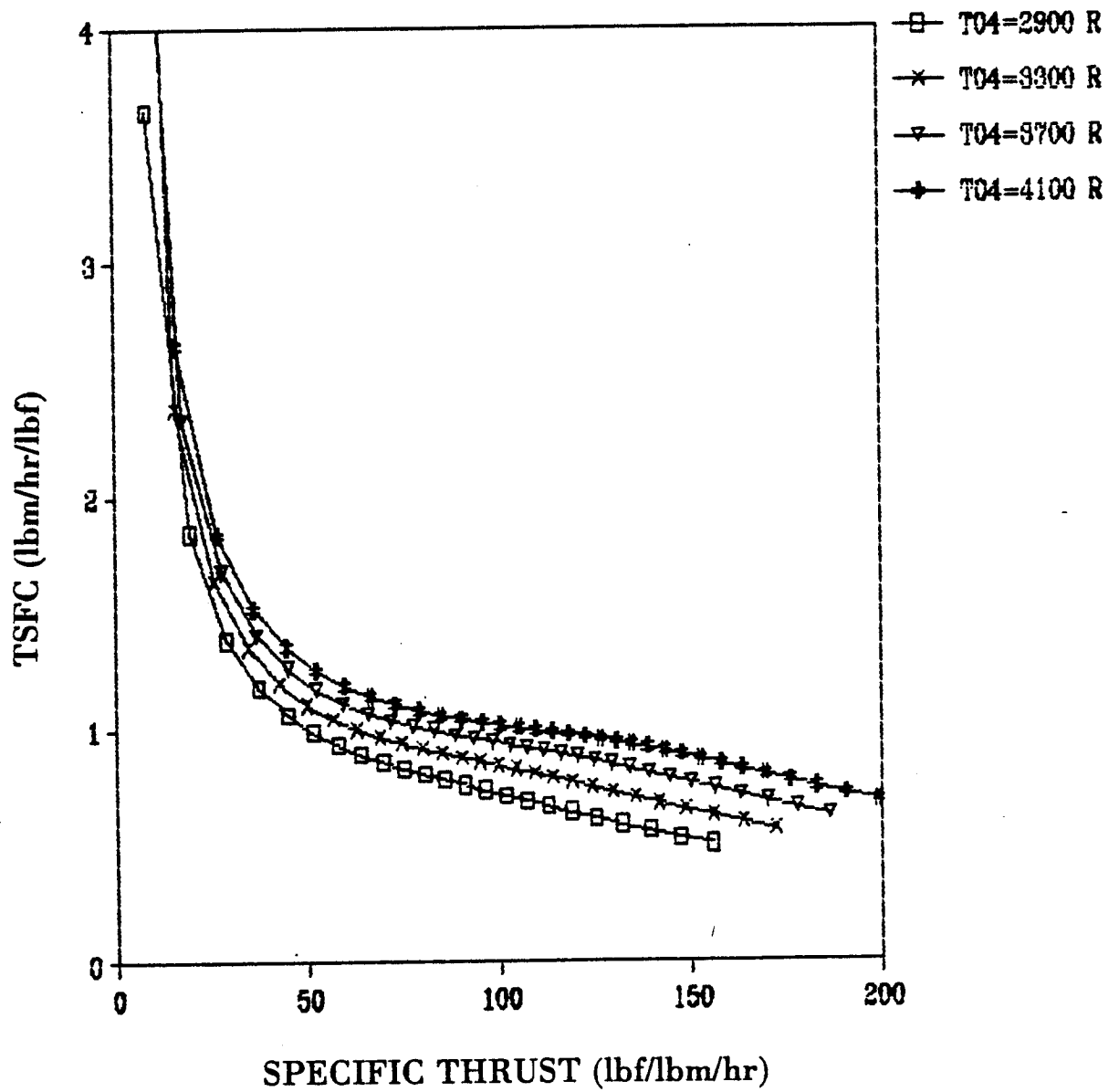


Figure 13. Thrust Specific Fuel Consumption Variation with Specific Thrust at Sea level and Different Combuster Temperatures (Bypass Ratio = 1.5)

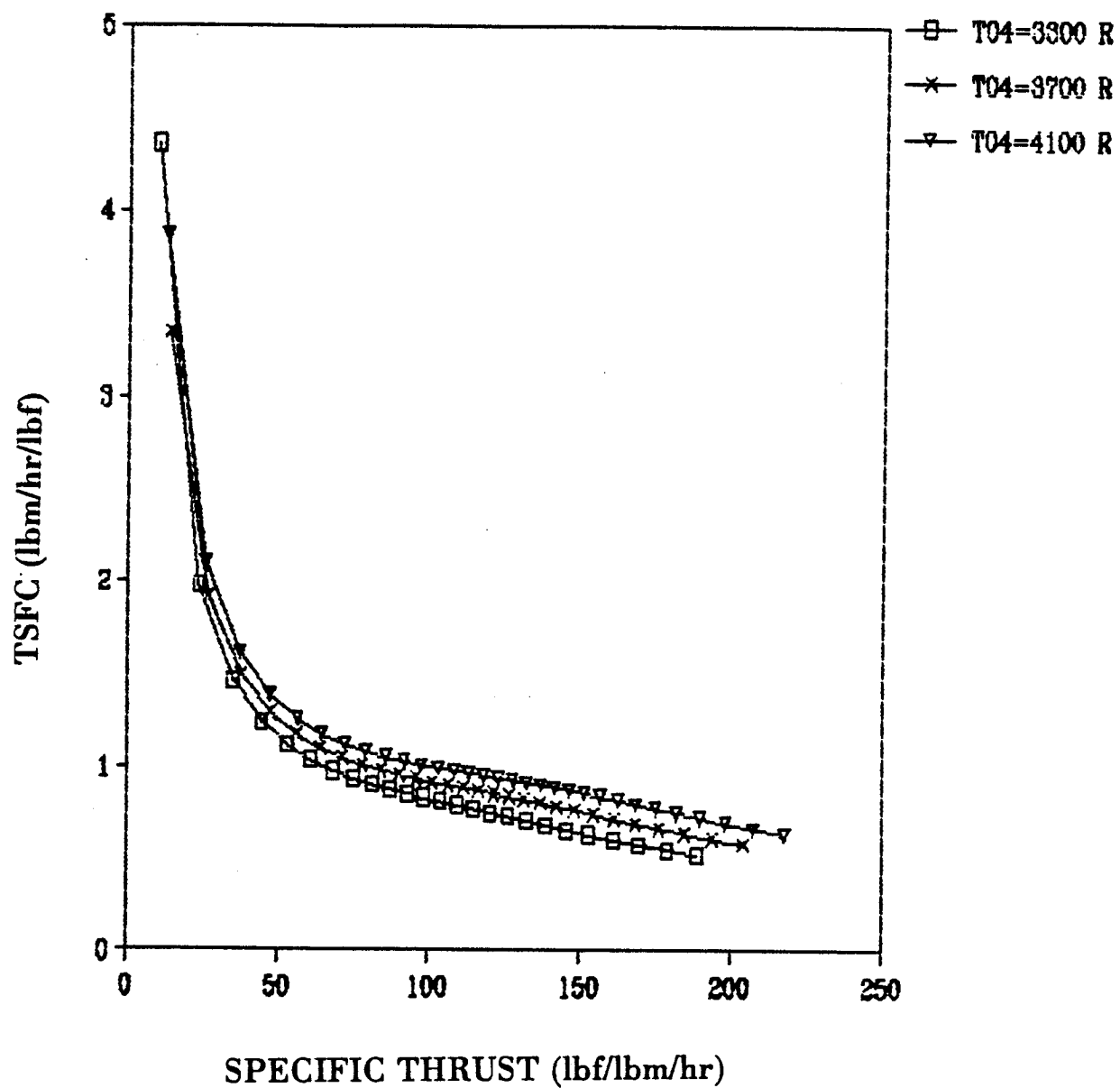


Figure 14. Thrust Specific Fuel Consumption Variation with Specific Thrust at Sea level and Different Combuster Temperatures (Bypass Ratio = 2.0)

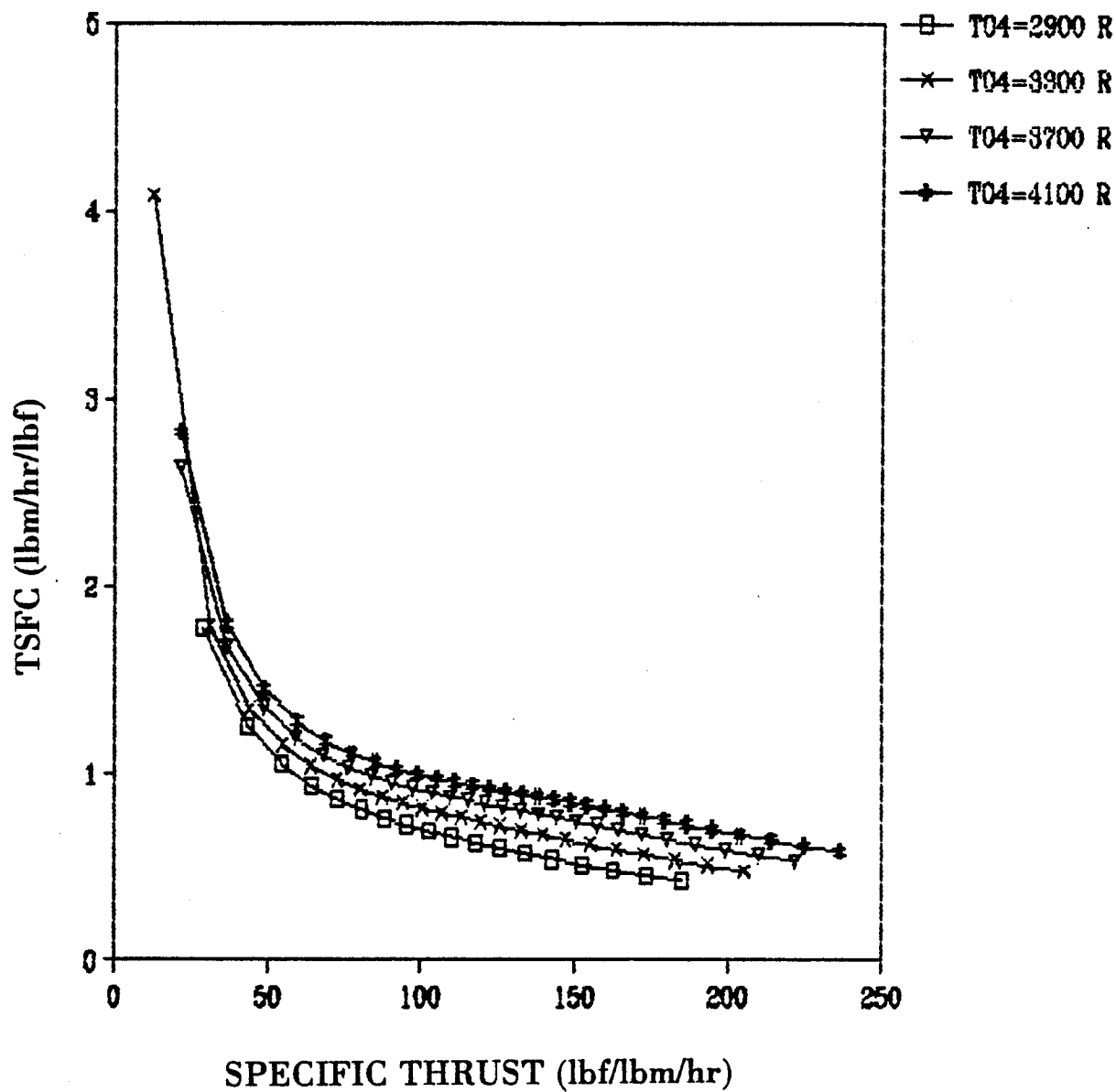


Figure 15. Thrust Specific Fuel Consumption Variation with Specific Thrust at Sea level and Different Combuster Temperatures (Bypass Ratio = 2.5)

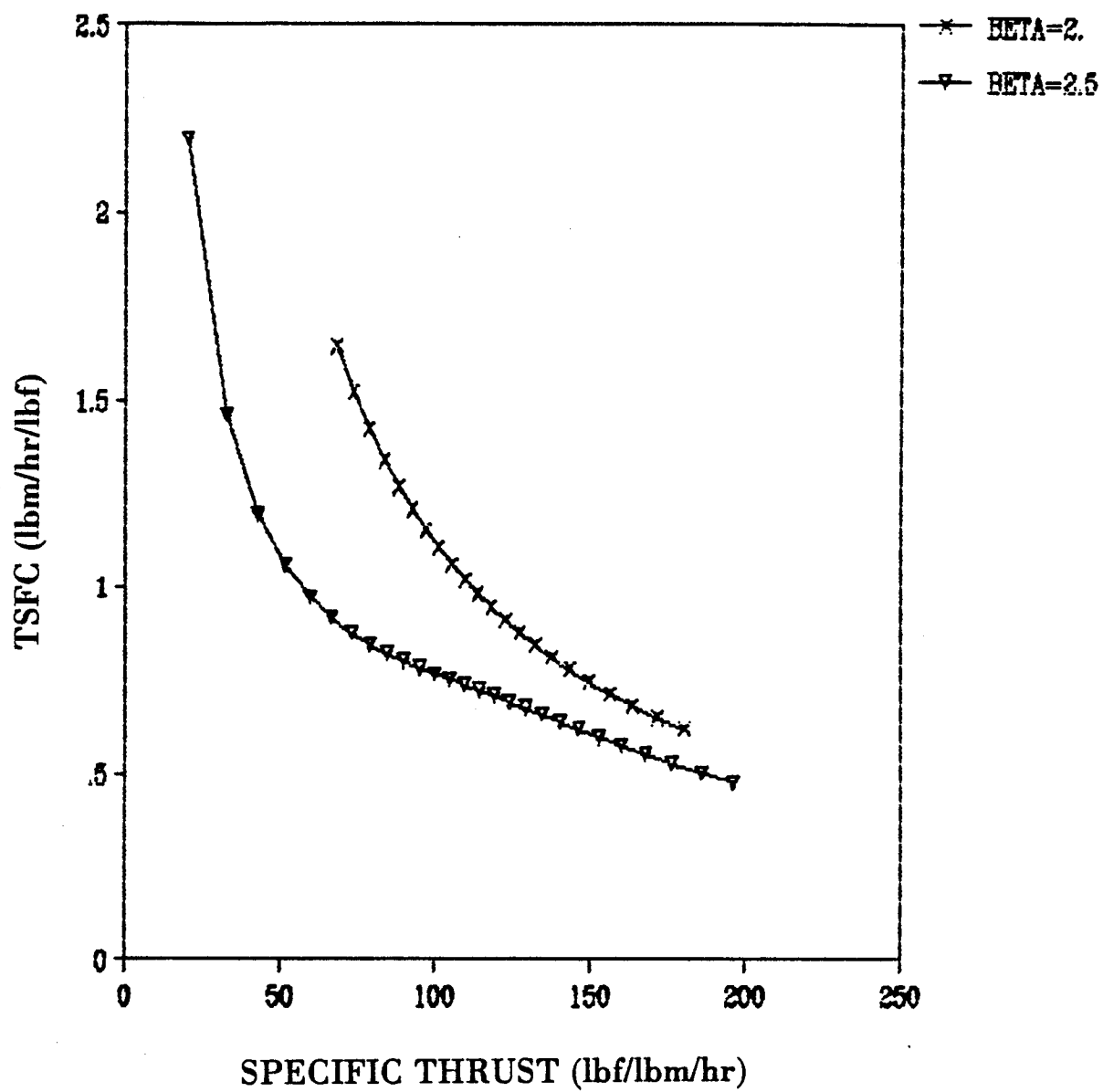


Figure 16. Thrust Specific Fuel Consumption at an Altitude of 45,000 feet at Different Values of Bypass Ratio

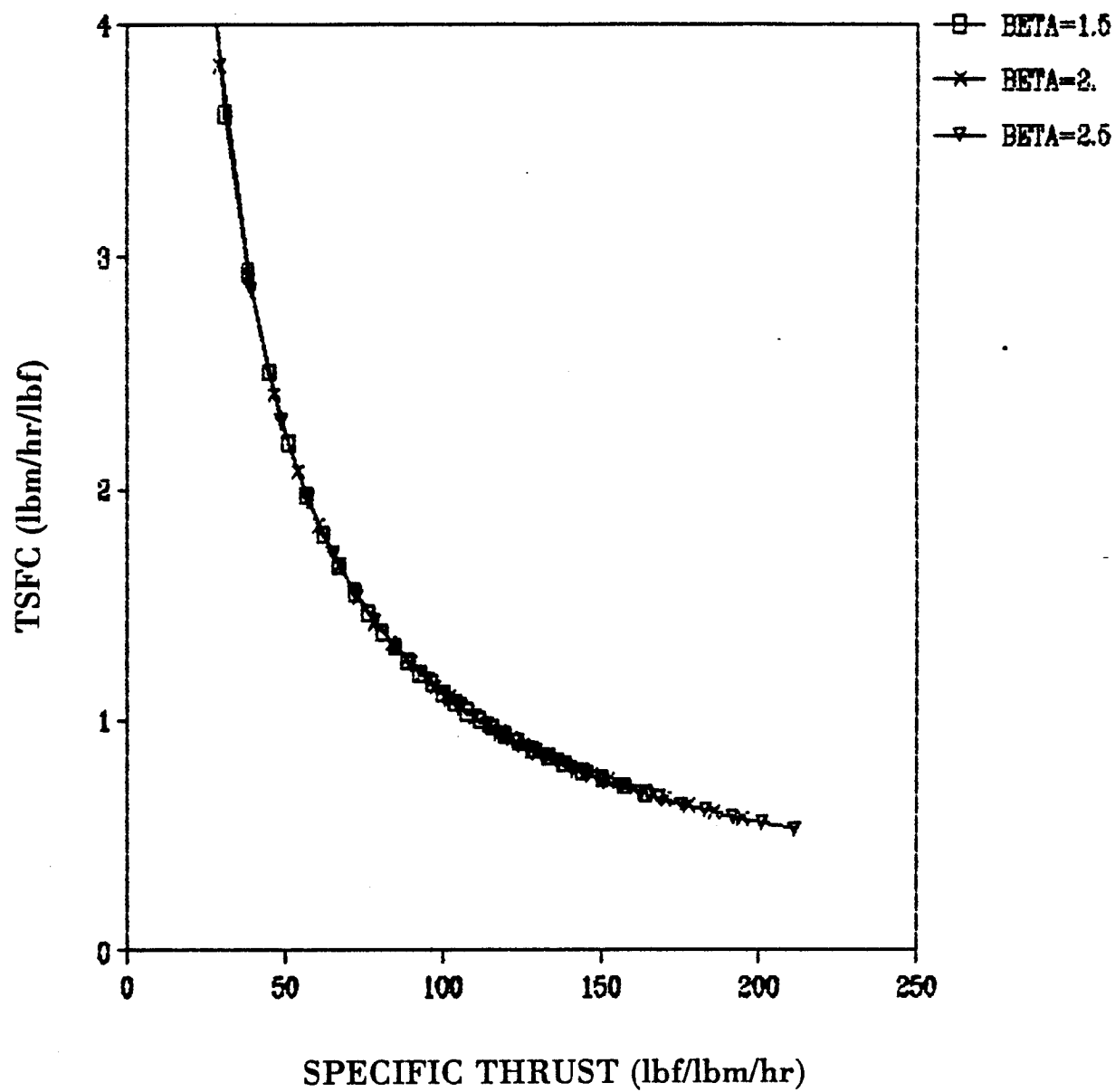


Figure 17. Thrust Specific Fuel Consumption at an Altitude of 70,000 feet at Different Values of Bypass Ratio

HIGH SPEED CIVIL TRANSPORT

STABILITY ANALYSIS

Aircraft stability characteristics are generally adversely affected by flight at high speeds and high altitudes. In reaching supersonics speeds, the HSCT will encounter several different aerodynamic flow regimes resulting in wide variations in stability and control characteristics. The center of gravity of the supersonic transport lies on the centerline of the aircraft at a location 139.8 feet from the nose; this position corresponds to 54.4 percent of the root chord. The center of gravity of the HSCT is calculated by determining the center of gravity of the various components of the vehicle.

Center of gravity locations for the wings, fuselage, nacelles, and vertical tail are calculated individually. The small wedge angle of the airfoil and the long root chord of the wing allow the wings to be treated as flat plates for simplicity of calculations. This is a valid assumption since the wing thickness is negligible in comparison to the wing length. The vertical tail can be treated in a similar fashion. The fuselage is roughly cylindrical in shape and allows the determination of the center of gravity by the approximation of a cylindrical shell. The nose is cone-shaped; therefore, its center of

gravity can be determined by the approximation of a conical shell. The nacelles are cylindrical in shape and the approximation of a cylinder is used to determine the center of gravity of the nacelles. The engines are assumed to be located at the center of the nacelles, and their weights are considered when determining the center of gravity of the nacelles.

Once the center of gravity for each component of the aircraft is determined, the moments due to the weight of each component are summed about the nose and the center of gravity for the entire aircraft can be determined. Since the HSCT is symmetrical about the centerline of the fuselage, the center of gravity is assumed to lie on the centerline. The assumptions made in calculating the center of gravity are based on basic geometric shapes; these assumptions are valid due to the simple geometric design of the HSCT.

Using the LOPROG Module for longitudinal stability analysis, the change in moment coefficient with respect to angle of attack is found to be negative for all flight regimes, indicating longitudinal static stability. This is to be expected since for a tailless aircraft, stability is obtained when the aerodynamic center is aft of the

center of gravity, as with the HSCT. Also from the LOPROG Module, the static margin is determined by dividing the change in moment with respect to angle of attack by the change in lift with respect to angle of attack. In this manner, the static margin is determined to range from a minimum of 1.86 feet at a Mach number of .58 to a maximum of 79.7 feet at a Mach number of 3.0.

For two-dimensional wings in subsonic flight, the aerodynamic center is located at roughly 25 percent of chord. As Mach number increases into supersonic range, the aerodynamic center shifts to roughly 50 percent of chord. Using data from LOPROG, the aerodynamic center for the HSCT lies at about 56 percent chord for subsonic flight and shifts to approximately 90 percent chord for supersonic regimes. The aerodynamic center is aft of the theoretical values due to the very high sweep angle and the very low aspect ratio of the wings.

The aft movement of the aerodynamic center will cause a nose down pitching moment. One method of correcting this is to use the flaps, but at supersonic speeds the problem is magnified and trimming the aircraft would require considerable control movement, resulting in a tremendous drag increase. An alternative to using

control surfaces is using fuel transfer to shift the aircraft center of gravity as the aerodynamic center shifts. As the HSCT accelerates to Mach 1, the fuel is pumped from the forward tanks to the rear tanks, thus moving the center of gravity aft to accommodate the shift in the aerodynamic center. As the aircraft slows to subsonic speeds, fuel would then be pumped back to the forward tanks.

Using fuel transfer to control the center of gravity location has two primary advantages. First, it will eliminate the need for large flap deflections for trimming the aircraft, thus avoiding the subsequent penalty in drag. Also, moving the center of gravity back during takeoff or landing would create the need to lower the flaps slightly, increasing the wing camber and thus increasing the lift at low speeds.

The requirement for yaw, or weathercock, stability is that C_{nb} must act to restore symmetric flight. At low speeds, the principal contributions to yaw stability come from the body and the tail. The effect of the fuselage may be estimated by the equation

$$C_{nb} = -1.3 \frac{\text{FUSELAGE VOLUME}}{S_b} \frac{h}{w}$$

and is calculated to be -.00503 for the HSCT. This destabilizing

contribution must be counteracted by vertical tails or propulsion components.

Since the HSCT will be required to operate in such a wide range of conditions, it will undergo almost constant changes in both static and dynamic stability characteristics. With such demands placed on the stability, the HSCT will require some type of artificial stability augmentation in order to maintain stability in all phases of flight.

HIGH SPEED CIVIL TRANSPORT

FLIGHT PROFILE

The design and performance characteristics of the HSCT call for a high-speed, long range flight profile. Over 50 percent of the gross takeoff weight of the HSCT is fuel, while only about 9.5 percent of the gross takeoff weight is payload. The takeoff profile requires a uniform acceleration from Mach .2 at sea level to Mach .85 at an altitude of 10,000 feet. The initial climb is followed by a constant velocity climb at Mach .85 to 45,000 feet, followed by an accelerated climb to the cruise speed and altitude. The cruise flight is to conclude with a constant glide angle of descent of 3 degrees.

The main objective of cruising at a high Mach number is to reduce travel time. Therefore, the fastest rate of climb is desirable in order to reach the cruise condition as soon as possible. Weight restrictions in the preliminary design will limit the amount of fuel carried on board the HSCT. Establishing an optimum climb profile will reduce the fuel consumption required for a fast climb to cruise condition.

Figure 18 is the flight profile for the HSCT. The mission of the HSCT is broken into 10 stages with 4 reserve stages. Each stage is analyzed and aircraft performance is described.

STAGE 1: Start-up, taxi, takeoff

The wing loading at takeoff is calculated to be 71.05 lb/ft², along with a thrust to weight ratio of 0.306. Using these values, the stall speed is computed to be 233.1 ft/s (158.95 mph) F.A.R. part 25 defines liftoff and climb speeds as 110% and 120% of stall speed respectively. Their values are $V_{LO}=260.2$ ft/s and $V_{CL}=279.7$ ft/s.

The total takeoff distance to clear a 50 foot obstacle is just over 9,000 feet and is calculated using the equation

$$S_{TOTAL} = \frac{W}{2g} \left(\frac{V_{LO}^2}{F_S - F_{TO}} \right) \ln \left(\frac{F_S}{F_{TO}} \right) + \frac{W}{2g} \left(\frac{V_{CL}^2 - V_{LO}^2}{T - D} \right) + \sqrt{h \left(\frac{W}{T - D} \right)^2 - 1}$$

The time for ground roll and climb-out over a 50 foot obstacle is approximately 46.7 seconds. Due to the good lifting properties of the double-delta wing and the ample thrust provided from the 4 STFF engines, the HSCT will not require a rotation during its ground roll. The rate of climb at takeoff calculated by optimizing the lift coefficient is 4,512 feet per minute. Using this value and the equation

$$\gamma = \sin^{-1} \frac{(R/C)_{TO}}{V_{CL}}$$

the climb angle needed at takeoff is determined to be 15.6 degrees.

STAGE 2: Climb to 10,000 feet at 250 knots

The second stage of the mission is a constant velocity climb to 10,000 feet. From an ACSL simulation, the thrust at the beginning of stage 2 is 51,977.9 lbs. with an aircraft weight of 677,467 lbs. This stage of the mission will last approximately 1.6 minutes and the HSCT will burn close to 3000 lbs. of fuel during the climb. At this point in the mission, the HSCT is 7.9 nautical miles down range.

STAGE 3: Accelerated climb to 45,000 feet

Stage 3 of the flight is an accelerated climb to 45,000 feet at the end of which the HSCT's velocity will be Mach 0.85. Stage 3 will carry the HSCT 17.6 nautical miles down range of the departure point and will last 1.63 minutes. The thrust, which was at 43,000 lbs. at the end of Stage 2, will be increased in a ramp type fashion to a maximum setting of 50,307 lbs. at an altitude of 37,824.9 feet. Thrust is now decreased in order to reach the value of Mach 0.85 at 45,000 feet. The rate of climb during this stage is around 360 ft/s. The HSCT weighs 674,514 lbs. at the beginning of Stage 3 and

671,136 lbs. at the end. This indicates that 3,378 lbs. of fuel are burned during Stage 3 and a total of 7,864 lbs. are burned to arrive at the end of this stage.

STAGE 4: Subsonic cruise for 150 nautical miles

The purpose of this portion of the mission is to place the HSCT well out over the ocean in order to begin the supersonic cruise portion of the flight. Stage 4 will take approximately 19 minutes to cover the specified range of 150 nautical miles. The aircraft will burn 19,757 lbs. of fuel during the cruise and will weigh 651,379 lbs. at the start of Stage 5.

STAGE 5: Accelerated climb to 70,000 feet

Stage 5 of the flight is the climb to 70,000 feet which is followed by the acceleration to cruise velocity of Mach 3.0. During this portion of the flight the aircraft climbs 24,614 feet and covers a ground distance of 32.37 nautical miles which places the HSCT 200 nautical miles down range. Thrust during the climb is increased from 25,775.1 lbs. to a maximum value of 55,808.1 lbs. at 48,487 feet. Thrust then levels off and decreases slowly to 53,495 lbs. for the

remainder of the climb to 70,000 feet. At the end of Stage 5 the aircraft has burned a total of 37,437 lbs. of fuel and has been flying for 25.91 minutes.

STAGE 6: Cruise at Mach of 3.0 at 70,000 feet

This stage covers the largest portion of the range and represents the most efficient portion of the mission. The weight of the HSCT at the beginning of supersonic cruise is 651,379.0 lbs. Stage 6 will last for 2.96 hours and span 5000.7 nautical miles. The aircraft is traveling only Mach 1.2 at the end of the climb to 70,000 feet but the flight velocity increases to Mach 3.0 in a period of 16.67 minutes and remains at Mach 3.0 for the remainder of the sixth stage. The thrust decreases slowly throughout this stage from an initial value of 50,050 lbs. to 12,248.7 lbs. at the end of cruise. The fuel used during this portion of the flight is 221,632 lbs. bringing the total fuel used at this point to 249,253 lbs. The weight of the HSCT at the end of the M 3.0 cruise is 429,747 lbs.

STAGE 7: Decelerate to M 0.85

This stage of the mission is designed to begin the descent to

landing for the HSCT. Stage 7 will begin at the 70,000 foot cruise altitude and end at 45,791 feet. An additional 343 nautical miles will be covered in this portion of the mission while 9484 lbs. of fuel are burned. Flight time for stage seven will be approximately 22 minutes.

STAGE 8: Subsonic cruise at M 0.83 for 150 nautical miles

Stage 8 is a subsonic cruise which will bring the HSCT to the vicinity of the airport. This cruise will take place at 45,791 feet and will burn 9483 lbs. of fuel. The total amount of fuel burned at the end of the eighth stage is 281,220 lbs. leaving an excess of fuel at this point of 68,780 lbs. Stage 8 will last 18.33 minutes during which time the thrust will be decreased from 21,287.4 lbs. to 10,212.1 lbs. The total range covered by the HSCT at the end of stage 8 is 5690.3 nautical miles which will bring the aircraft to the beginning of its 30 minute loiter over the airport.

STAGE 9: 30 minute loiter

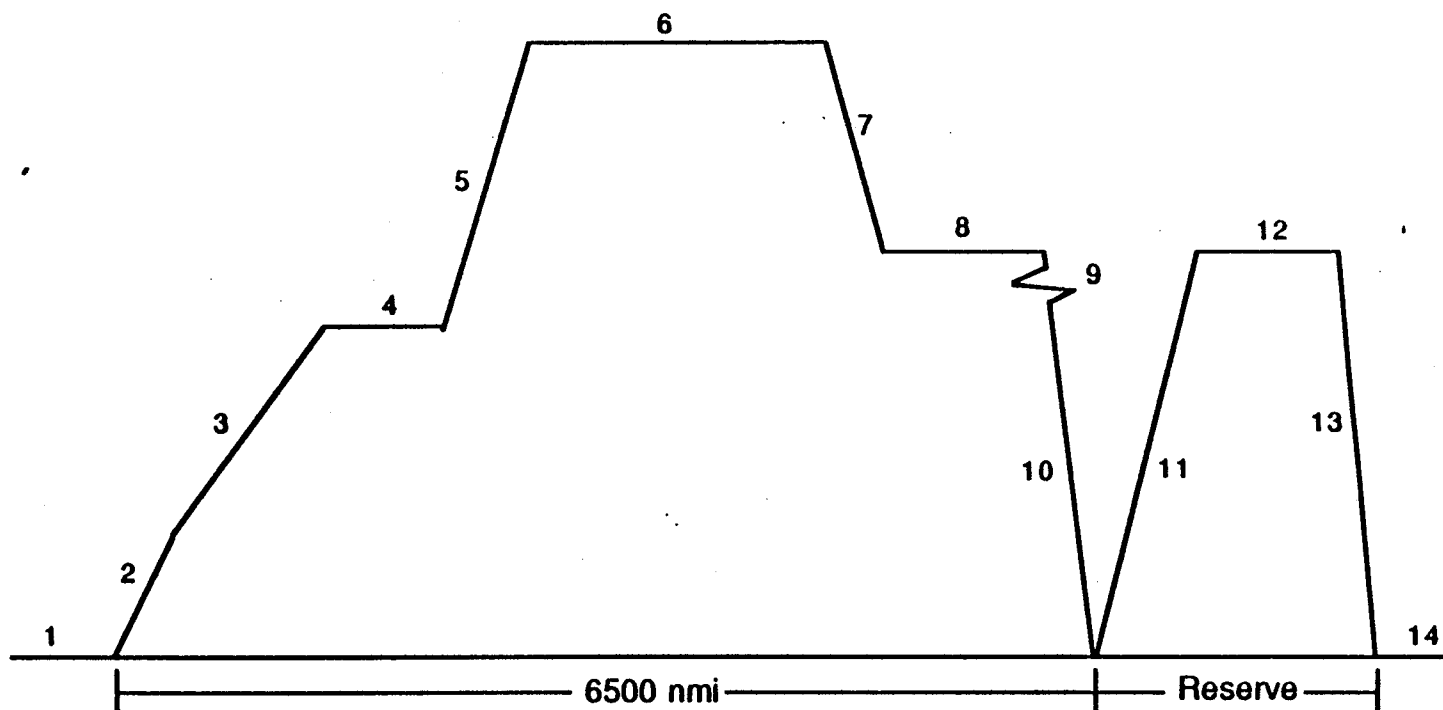
Stage 9 is a 30 minute loiter over the airport at which time the

HSCT will obtain instructions and clearance for descent and landing. The loiter will take place at 45,791 feet and will burn 17,908 lbs. of fuel. Mach number during the loiter will be decreased from the cruise value of M 0.83 to M 0.59 and the thrust will be maintained at around 15,000 lbs. after the mach number is reduced.

STAGE 10: Descend to 1,500 feet

This stage takes place after the loiter and is the descent to the airport or to the beginning of the reserve mission. The descent will take approximately 11 minutes and will reduce the weight of the HSCT to 379,774 lbs. A total of 50,774 lbs. of fuel will be left for the reserve mission which is more than enough to span the 800 nautical mile range of the reserve mission.

Figure 18. Flight Profile for the HSCT



1. Start-up, taxi, takeoff
2. Climb to 10,000 ft. at 250 knots
3. Accelerate to $M = .83$, climb to 45,000 ft.
4. Subsonic Cruise ($M = .83$, 150 nmi)
5. Climb and accelerate to $M = 3.0$, 70,000 ft.
6. Cruise at $M = 3.0$, 70,000 ft.
7. Decelerate to $M = .83$, 150 nmi

8. Subsonic Cruise at $M = .83$, 150 nmi
9. 30 minute loiter
10. Descend to 1,500 ft.
(Start Reserve Mission)
11. Climb to 45,000 ft.
12. Subsonic Cruise ($M = .83$, 300 nmi)
13. Descend to 1,500 ft.
14. Landing, taxi, shutdown

*SUMMARY AND
CONCLUSIONS*

The High Speed Civil Transport will carry three-hundred passengers on trans-pacific flights at speeds up to Mach 3. The aircraft uses a simple double delta wing configuration. The double delta also helps keep body drag at a minimum which is an important characteristic.

Since the aerodynamic center moves around during flight from subsonic to supersonic and visa-versa, some control over the center of gravity is needed. The control will come from the shifting of fuel between the main fuel tank and the front trim tank or rear trim tank depending on the type of movement desired.

Four supersonic through-flow fan engines and their nacelles are integrated into the wing to help reduce wave drag. This type of engine will act as a conventional turbofan engine during takeoffs and subsonic cruise. It will, then, approach a turbojet cycle at supersonic speeds. Compared to other engines, the STFF has a shorter inlet, a simpler single stage fan, and a lighter, simpler nozzle.

The HSCT combines existing technology with the expectations of future breakthroughs in many of the areas governing supersonic

flight, especially in materials. Materials for this type of aircraft need to be very light and resist high temperatures while still being very strong. By developing this type of a passenger transport the United States will remain and even become stronger in aerospace industry. Also, the HSCT will provide a means of trans-pacific flight for people without wasting a great amount of time and creating serious jet lag.

BIBLIOGRAPHY

1. Babister, A. W.; International Series of Monographs in Aeronautics and Astronautics. Division VI: Flight Testing; Pergamon Press; 1961.
2. Baily, Roy; "Evolution of the Lockheed Supersonic Transport", Lockheed Horizons; Spring, 1965.
3. Barnhart, Paul J.; A Preliminary Design Study of Supersonic Through-Flow Fan Inlets; AIAA 88-3075, 1988.
4. Birtles, Philip; Concorde; Ian Allan Ltd.; 1984.
5. Boyd, R., Gregorek, G., and Weiseman, P.; "High-Speed Transpacific Passenger Flight", AIAA; 1988.
6. Champagne, G. A.; Payoffs for Supersonic Through Flow Fan Engine in High Mach Transports and Fighters; AIAA 88-2945, 1985.
7. Corning, Gerald; Supersonic and Subsonic CTOL and VTOL Airplane Design; 1976.
8. CRC Standard Mathematical Tables; CRC Press; 1981.
9. Davis, John G. and Dixon, S.; "Beyond Simulation", Aerospace America; July 1988.
10. DeMeis, Richard; "An Orient Express to Capture the Market", Aerospace America; September, 1987.
11. Etkin, Bernard; Dynamics of Flight-Stability and Control; John Wiley & Sons Inc.; 1982.
12. Hale, Francis J.; Aircraft Performance, Selection, and Design; John Wiley & Sons Inc.; 1984.

13. Heppe, Richard and Englebery, Channing; "Supersonic Transport Design Evolution", Lockheed Horizons; Second Quarter, 1966.
14. Hexcel Corp.; "The Basics on Sandwich Construction", Report No. TSB 124.
15. Howard, Lee and Williams, James; "SST Prospectus-Economics of the United States Supersonic Transport", Lockheed Horizons; Autumn, 1965.
16. Kuethe, Arnold M. and Chow, Chuen-Yen; Foundations of Aerodynamics; John Wiley & Sons Inc.; 1986.
17. Larson, Ken; To Fly the Concorde; Tab Books Inc.; 1982.
18. Loomis, James P.; High-Speed Commercial Flight; 1986.
19. McDonald, John; "SST Maintenance and Ground Ops", Lockheed Horizons; Second Quarter, 1966.
20. Meriam, J.L. and Kraige, L.G.; Engineering Dynamics, John Wiley & Sons, Inc. 1986.
21. Nihart, Gene L. and Brown, Jeffrey J.; Supersonic Propulsion Systems and Community Noise Suppression Concepts; AIAA 88-2986, 1986.
22. Ott, James; "High-Speed Transport Study Focuses on Lower Mach Range", Aviation Week & Space Technology; January 29, 1988.
23. Owens, Kenneth; Concorde: New Shape in the Sky; Jane's Publishing Co.; 1982.

24. Powers, Albert G.; "Supersonic Propulsion Technology"; Aeropropulsion 1979: NASA Conference Publication 2092, May 1979; pp. 345-358.
25. Sakma, T.F. and Davis, G.W.; "Advanced Structures Technology Applied to a Supersonic Cruise Arrow Wing Configuration", Proceedings of the SCAR Conference.
26. Shevell, Richard S.; Fundamentals of Flight, Prentice-Hall, Inc. 1989.
27. Sweetman, Bill; Aircraft 2000: The Future of Aerospace Technology, The Military Press, 1984.
28. Taneja, Nawel K., Heath, D. and Co.; The International Airline Industry; 1988.